Investigation of the thermo-mechanical and ablative behaviour of silicon carbide based concretes exposed to hybrid propulsion environments

Raffaele d'Elia, Gérard Bernhart, Thierry Cutard, Gilles Peraudeau, Marianne Balat-Pichelin

IAC-13, C2,4.6x17408

INVESTIGATION OF THE THERMO-MECHANICAL AND ABLATIVE BEHAVIOUR OF SILICON CARBIDE BASED CONCRETES EXPOSED TO HYBRID PROPULSION ENVIRONMENTS

Raffaele D'ELIA[1, 2]

Gérard BERNHART [2], Thierry CUTARD [2], Gilles PERAUDEAU [3], Marianne BALAT-PICHELIN [3]

[1] CNES – Direction des Lanceurs, 52 rue Jacques Hillairet, 75612 Paris Cedex
[2] Université de Toulouse; Mines Albi, INSA, UPS, ISAE, ICA; Campus Jarlard, F-81013 Albi cedex 09, France
[3] PROMES-CNRS, 7 rue du four solaire, 66120 Font-Romeu Odeillo, France

ABSTRACT

This research is part of the PERSEUS project, a space program concerning hybrid propulsion and supported by CNES. The main goal of this study is to characterize silicon carbide based micro-concrete with a maximum aggregates size of 800 μm, in a hybrid propulsion environment. The nozzle throat has to resist to a highly oxidizing paraffin/LOX hybrid environment, under temperatures ranging up to 3000°C.

The study is divided in two main parts: the first one deals with the thermo-mechanical characterization of the materials up to 1400°C and the second one with an investigation on the ablation behaviour in a standard atmosphere, up to 3000°C. The combustion time is of 15s.

Young's modulus was determined by resonant frequency method: results show an increase with the stabilisation temperature. Four points bending tests have shown a rupture tensile strength increasing with stabilisation temperature, up to 1200°C. Sintering and densification processes are primary causes of this phenomenon. Visco-plastic behaviour appears at 1100°C, due to the formation of liquid phases in cement ternary system.

High-temperature oxidation in ambient air was carried out at PROMES-CNRS laboratory, on a 2 kW solar furnace, with a concentration factor of 15,000. A maximum 15 MW/m^2 incident solar flux and a 7 to 90 seconds exposure times have been chosen. Optical microscopy, SEM, EDS analyses were used to determine the microstructure evolution and the mass loss kinetics. During these tests, silicon carbide undergoes active oxidation with production of SiO and CO smokes and ablation. A linear relation between mass loss and time is found. Oxidation tests performed at 15 MW/m^2 solar flux have shown a mass loss of 20 mg/cm^2 after 15 seconds. After 90 seconds, the mass loss reaches 80 mg/cm^2.

Surface temperature measurement is a main point in this study, because of necessity of a thermo-mechanical-ablative model for the material. Smokes appear at around 6.5 MW/m^2, leading to the impossibility of useful temperature measurements by optical pyrometry.

Micro-concrete is really interesting for the nozzle realisation, thanks to its workability, and its thermo-mechanical properties. After 30 seconds, mass loss in micro-concrete is one half of pure α-SiC. This result is really interesting to study SiC-based concretes in oxidizing environments, instead of pure SiC. Our goal is to improve the thermo-mechanical properties and to study micro-concrete in a hybrid propulsion environment, developing a phenomenological model.

I. INTRODUCTION

SiC-based ceramics are very interesting materials for high temperature space applications, because of SiO_2 scale formed in passive oxidation conditions, with a parabolic mass gain. The reaction that occurs is the following:

$$SiC(s) + \frac{3}{2}O_2(g) = SiO_2(s) + CO(g) \qquad (1)$$

However when oxygen partial pressure is lower than the stability value [1], that depends on temperature and pressure conditions, the SiC substrate undergoes rapid active oxidation, with formation of gaseous products and linear mass loss [2]. The reaction in this domain is the following:

$$SiC(s) + O_2(g) = SiO(g) + CO(g) \qquad (2)$$

At 1340°C calcium aluminate cement [3], that binds SiC aggregates in concrete, forms a fluid vitreous phase in the CaO-Al_2O_3-SiO_2 (CAS) ternary system [4]. In real, cement sulphates and carbonates together have low melting point eutectics, of order of 800°C-900°C [3]: this transient melting is quantitatively ephemeral, but it is important for cement sintering and densification. At 1340°C, when cement eutectics appear, the liquid quantity abruptly rises from zero to a significant value, in the range of 15-25% [3]. These phases could protect SiC aggregates during active oxidation, delaying the oxidation process and reducing mass loss. In fact, oxygen would have to diffuse through cement, liquid phases and aggregates, increasing ablation heat and slowing recession rate.

The aim of this study, part of the PERSEUS project, launched by CNES in 2006, is to characterize a particular SiC-based refractory concrete in a hybrid propulsion environment and to finally manufacture a complete nozzle, for tests at ONERA, France.

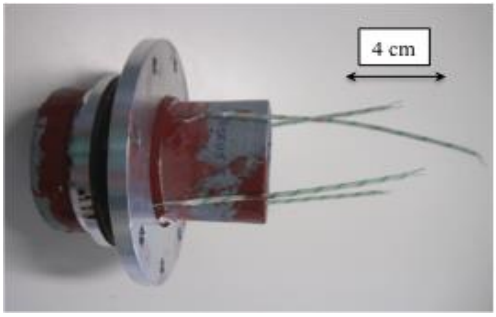

Fig. I: PERSEUS nozzle in refractory concrete, with silica insulating material, aluminium carter and four K-type thermocouples.

Concrete will be exposed to a very oxidizing environment, at 2 MPa total pressure with temperatures up to 3000°C and for a very limited time (15s). Exhaust gases produced by hybrid rocket contain more oxidizing chemical species than VEGA solid booster: 11.2 mol% CO_2 (against 1.2 mol%), 32.0 mol% H_2O (against 11.8 mol%) and 0.6 mol% O_2 (against 0.0 mol%). From here the idea is to use SiC-based refractory concrete that is less reactive than graphite used in others similar CNES projects. Moreover concrete processing route is really simple, and allows a nozzle manufacturing in only one piece.

To save time and resources in the product development, relatively simple approaches should be tried, like the use of concrete type materials. Its utilization is an attractive alternative. Compared to metallic materials, a cooling system is not necessary, because of different types of heat dispersion: smoke generation, liquid phases formation, vaporization and oxidation.

Ablation heat quantifies all these phenomena. Our purpose is to understand ablation, oxidation of concrete and to measure mass loss as a function of time.

II. MATERIALS AND METHODS

II.I Concrete properties

The chemical composition of the concrete used in this study is shown in Table I. In this material, SiC is the main component, with a maximum aggregates size of 800 µm. This aggregates size is not common in concrete; for this reason this material has been renamed *micro-concrete*.

According to triple weighing measurement [5], after stabilization at 1200°C, material density is 2.49 g/cm^3, with an open porosity of 17.06 vol%. Nominal open porosity at 800°C is 21vol% [6]. This important difference is linked to liquid phases produced between 800°C and 1200°C, with cement sintering and with the associated densification [7].

Chemical species	Average composition	80-800µm (60 wt%)	<80µm (40 wt%)
SiC	80.0 wt%	100 wt%	50.0 wt%
Al_2O_3	14.0 wt%	-	34.0 wt%
SiO_2	5.0 wt%	-	13.0 wt%
CaO	1.4 wt%	-	3.5 wt%

Table I: Chemical composition of micro-concrete [6].

A thermal conductivity of 12.8 W/mK at 17°C was measured by the hot disk method.

Figure II shows concrete microstructure: SiC aggregates are light grey and irregular, surrounded by the cement matrix (darker parts).

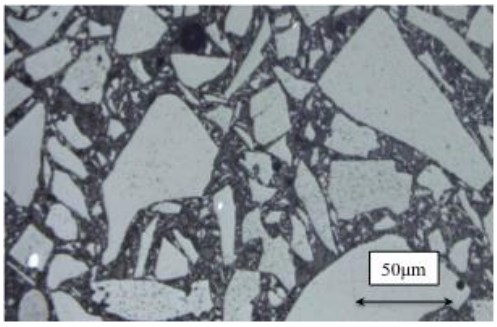

Fig. II: Microstructure of SiC-based micro-concrete, fired at 1200°C during 5 hours.

A high alumina cement, used as binding agent, ensures good mechanical properties to concrete, while SiC aggregates give its refractoriness [4].

During first stabilization cycle, cement undergoes several microstructural evolutions: dehydration (20°C-300°C), recrystallization (440°C-900°C), eutectic liquid phases formation, sintering and densification (800°C-1500°C) [4], with a change in thermo-mechanical properties. All cement microstructural transformations are known as conversion. Several studies have been made on this topic [7]. Conversion can be divided in three parts: in *first conversion* (20°C-800°C), concrete undergoes thermal damage, connected to mismatch of expansion behaviour between cement matrix and aggregates, which results in lower Young's modulus. In this domain the concrete has a damageable elastic behaviour; in *transition domain* (800°C-1000°C) concrete ceramization begins, continuing in *third conversion* (1000°C-1500°C), with a visco-plastic behaviour, driven by the development of eutectic liquid phases. Rupture of the concrete is always quasi-brittle [7].

Stabilization temperature	E at 20°C (GPa)	σ_R (0.2 mm/min) (MPa)			σ_R (0.02 mm/min) (MPa)
		20°C	1100°C	1200°C	1200°C
700°C	40	-	-	-	-
900°C	70	14	17	16	13
1200°C	75	27	29	25	18

Table II: Thermo-mechanical properties of micro-concrete: Young's modulus at 20°C and bending strength at 20°C, 1100°C and 1200°C. At 1200°C tests were performed at two crosshead speeds, to exhibit the visco-plastic effect.

Thermo-mechanical properties of micro-concrete are shown in Table II: Young's modulus and rupture bending strength increase with stabilization temperature, due to increasing densification and sintering of concrete at higher stabilization temperatures.

Bending strength has been measured using a thermo-mechanical testing machine MTS 50kN and an AET oven to reach testing temperature (1600°C maximal temperature). Young's modulus values have been obtained by resonance frequency method [8].

II.II Concrete processing route

Refractory concretes are unshaped materials. To ensure aggregates binding, cement has to follow a processing route to allow hydraulic bond formation. The micro-concrete used in this study is *calcium aluminate cement*, which contains almost 70 wt% of alumina. The hydraulic bond is formed when mixing water is added to cement. Water quantity is calculated to ensure perfect equivalence with reactive phases in cement: C_3A, $C_{12}A_7$, CA, CA_2, CA_6. Each phase has a different reactivity with water to form hydrates, which depends upon C/A ratio. In particular the first two phases (C_3A and $C_{12}A_7$) dissolve immediately in water, while the three others (CA, CA_2, CA_6) are more stable [4].

Micro-concrete requires 8.3 wt% of water, that is mixed with concrete during 6 minutes. Then, concrete is poured in 25x25x150 mm^3 mould, locked on a vibrating table to reduce concrete porosity. Concrete is then stabilized under plastic film during 48 hours at 20°C, to ensure correct hydration and to avoid water evaporation. Plastic film prevents different evaporation between the top and the core of the sample. Concrete is then placed in oven at 110°C during 24 hours, to ensure complete water evaporation. Finally samples are fired at 1200°C during 5 hours. Temperature ramp is really important, because of spalling or explosions phenomena if it is too fast. Normal temperature ramp is 100 °C/hour [7]. After cooling, samples are cut with diamond saw. Figure III shows a sample before test at the focus of a 2 kW solar furnace.

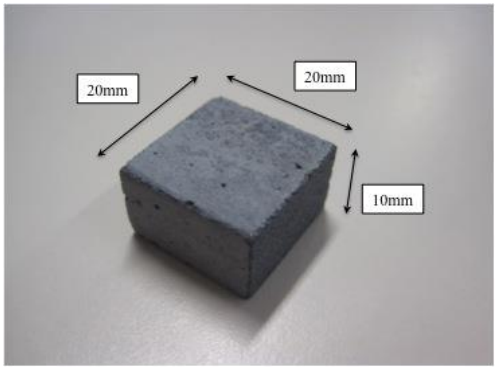

Fig. III Micro-concrete sample used in solar furnace tests. Dimensions are 20x20x10 mm^3.

II.III Solar furnace facility

The 2 kW *Medium Size Solar Furnace* (MSSF) test facility (Fig. IV) is used to characterize micro-concrete at very high temperature, measuring mass loss as function of time and for different concentrated solar flux. All tests were done at 84 kPa total air pressure, which is the standard value at PROMES laboratory located at 1500 m altitude.

Fig. IV Solar furnace facility, during a test.

The heliostat, a mobile mirror that follows the apparent movement of the sun during the day, reflects sun radiation towards a 2 m parabolic mirror with a focal length of 851 mm, which concentrates solar power to its focus. A shutter is placed between the heliostat and the parabolic concentrator in order to control the solar flux level. The sample-holder is water-cooled [9].

The material surface temperature is measured using a blind-solar monochromatic (5 μm) pyrometer, with a focal length of 490 mm and an analysis spot diameter of 1.7 mm.

The solar flux absorbed (ϕ_{abs}) by the material is calculated according to the following expression:

$$\phi_{abs} = \alpha_M \cdot S \cdot F \cdot E_S \quad (3)$$

where α_M is the solar absorptivity, depending on the material properties, S is the surface exposed to the solar flux, F is a concentration factor, depending on the mirrors, E_S is the direct solar flux measured using a pyrheliometer.

Solar absorptivity has been measured by FT-IR technique

This expression can be rearranged dividing by the surface and merging F and E_S:

$$q_{abs} = \alpha_M \cdot q_e \quad (4)$$

where q_{abs} is the absorbed solar flux (ϕ_{abs}/S) and q_e is the concentrated solar flux ($F \cdot E_S$).

Concentrated solar flux is a Gaussian function, with a maximum value of 15 MW/m^2 for a 1000 W/m^2 direct solar flux. The concentration factor is 15000 for this solar furnace facility.

Micro-concrete can be heated up to 1900°C, for a concentrated solar flux of 6.5 MW/m^2. Above this level, smokes composed of SiO and CO gases and SiO_2 particles produced by re-condensation are generated and the pyrometer cannot be used anymore. Smokes hinder measurement and could damage the instrument lens. This is a focal point in this work: thermocouples are used to measure values inside the material to finally obtain its absorption coefficient. Mass loss measurements obtained by weighing - before and after test - are performed with a resolution of 0.1 μg. Post-test characterizations of the materials are carried out using SEM and optical microscopy.

III. RESULTS AND DISCUSSION

III.I SiC and concrete active oxidation

6H α-SiC samples (from Boostec now Mersen, France) have been tested during 30 seconds for different concentrated solar fluxes: Figure V shows samples tested at 7.5 MW/m^2 (a) and 15 MW/m^2 (b). Samples have been placed on the top of a concrete sample to reach high temperature values and to reproduce similar concrete test conditions. Compared to micro-concrete, conductivity of this 6H α-type silicon carbide is 14 times greater (180 W/mK vs. 12.8 W/mK). To recreate similar temperature conditions and observe the same phenomena, this configuration has been chosen.

First tests showed SiC active oxidation, with smokes generation and a mass loss of 20.5 mg/cm^2. Smokes amount is really limited and passive-to-active transition appears, with SiO_2 scale breakdown. Hinze and Graham [2], Turkdogan et al. [10], Heuer and Lou [11], Balat et al. [12–16] have discussed passive-to-active oxidation transition in SiC. Passive oxidation is characterized by the presence of a SiO_2 protective scale without bubbles and active oxidation is characterised by the presence of bubbles on the surfaces, and/or silica layer damage (SiO_2 decomposition and CO emission) or bare SiC surface according to the oxygen partial pressure and temperature conditions [12–16]. When tested under 12 and 15 MW/m^2 SiC samples show SiO_2 re-deposition after stopping the solar flux due to the reaction between SiO smoke and the oxygen of the surrounding atmosphere and the deposit is mainly present in the colder area.

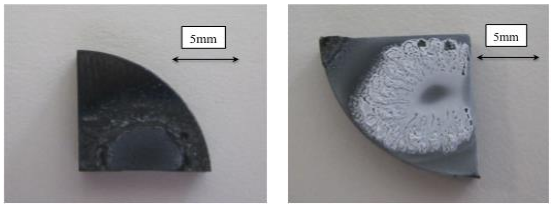

(a) (b)

Fig. V Sintered 6H α-SiC tested at (a) 7.5 MW/m^2 and (b) 15 MW/m^2 during 30 seconds.

Similar observations can be done on SiC-based concrete. Figure VI shows three samples exposed to 15 MW/m^2 during 7, 30 and 90 seconds. Crater diameter increases with exposure time. All samples show silica deposition on the outer region, like for pure SiC, and liquid phases solidified at the edge of the crater. Central zone after 7 and 30 seconds shows condensed liquid phases. Sample tested during 90 seconds shows a crater more pronounced in the central zone and a darker edge zone. Heat conduction transfers energy through the thickness towards the water-cooled sample-holder. Another part of this energy is dispersed by convection and surface radiation. Moreover heat conduction allows tangential heat transfer: this is the reason why the crater diameter increases with time.

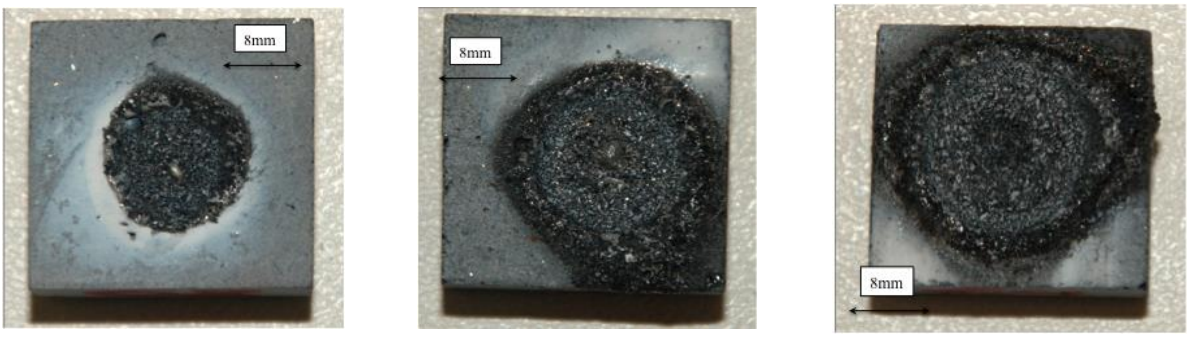

(a) (b) (c)

Fig. VI SiC-based concrete samples tested at 15 MW/m^2, during 7 seconds (a), 30 seconds (b) and 90 seconds (c).

III.II Mass loss in concrete and in pure α-SiC

Different tests have been made on micro-concrete to study its behavior in active oxidation conditions. Micro-concrete has been tested at 9, 11, 12 and 15 MW/m^2 solar flux, during 7, 15, 30, 60 and 90 seconds. In these conditions, smokes are generated and it is possible to evaluate the mass loss by weighing. Absolute mass loss is divided by the ablated surface area, measured by caliper: 2 diameters are measured, because of elliptic form of the crater. 2D profilometry is under study to improve the measurement accuracy.

Figure VII shows the results for pure α-SiC that has been tested during 30 seconds and for micro-concrete samples under three concentrated solar fluxes: 7.5, 12 and 15 MW/m^2. For the micro-concrete, linear trends interpolate results at different fluxes. The mass loss is increasing with the concentrated solar flux and with time. Pure α-SiC shows higher mass loss than micro-concrete at 12 and 15 MW/m^2 for 30 seconds exposure. This observation is really interesting and can be explained by the formation of eutectic liquid phases, since 1340°C. These phases protect SiC aggregates, making more difficult the interaction with atmospheric oxygen and reducing mass loss with respect to pure α-SiC. The behavior observed for α-SiC and for micro-concrete shown in Figure VII is clearly an example of silicon carbide active oxidation, with smokes generation and mass consumption.

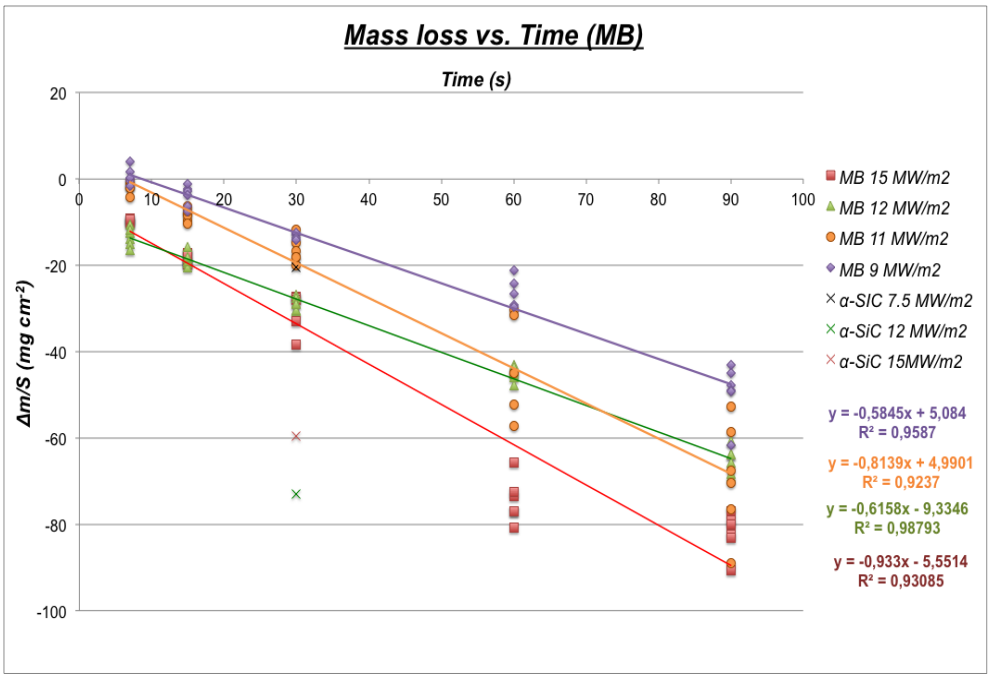

Fig. VII Mass loss curves for different exposure duration and concentrated solar flux for α-SiC and micro-concrete (MB).

Linear behavior is explained by Hinze and Graham [2] and Balat et al. [12–16] that extended to silicon carbide Wagner theory on silicon active oxidation [1]. They studied active oxidation of SiC exposed to different pressure values, seeing that active oxidation gives a linear mass loss.

In our active oxidation conditions, surface temperature is not measurable directly, because of smokes generation that prevents the use of pyrometer. For this reason, temperature measurement by indirect method is under study.

III.III Temperature measurements

Pyrometric measurements have shown an increasing value of the surface temperature with the concentrated solar flux. Experimental measurements have been made with the blackbody hypothesis (emissivity=1) set in the Heitronics KT15 pyrometer. Afterwards, temperature values have been corrected using Planck's law taking into account a spectral (5 µm) normal emissivity for the micro-concrete of 0.9 independent of temperature that is a likely value as the spectral normal emissivity of SiC (80% content of the micro-concrete) is few temperature dependent.

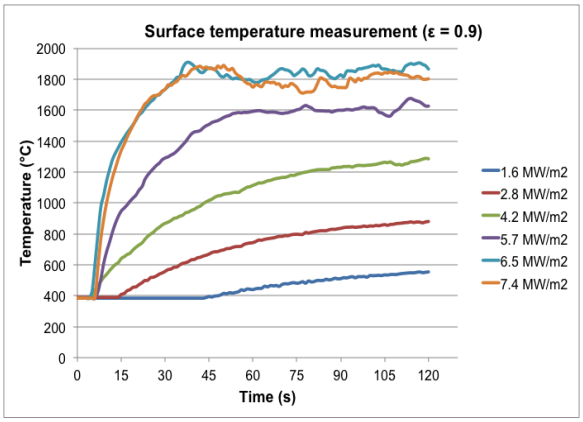

Fig.VIII Surface temperature measurement by optical pyrometry for concentrated solar flux from 1.6 to 7.4 MW/m^2.

Figure VIII shows the corrected values of surface temperature measure by optical pyrometry. Temperature increases with time up to an asymptotic value after 90 seconds. Between 1.6 and 5.7 MW/m^2 the surface temperature increases regularly. Above 5.7 MW/m^2 smokes generation begins and above 6.5 MW/^{2} it is not possible to measure surface temperature anymore due to the intense smokes generation. This maximum asymptotic value could be due to the zero transmission (at 5 µm) of SiO_2 particles that can be found due to re-condensation and/or reaction of SiO with the surrounding O_2 in the smokes above the sample. For this reason, this optical pyrometer cannot be used for solar fluxes greater than 6.5 MW/m^2. Smokes generation also reduces the amount of solar flux reaching the micro-concrete surface, thus reducing the surface temperature. Moreover, measurements under 390°C is not possible because of instrument sensibility and the highest surface temperature measured is of 1900°C due to smokes limitation and not to the pyrometer.

This problem could be solved with the immersion of thermocouples inside the samples. Measurement inside the material can allow COMSOL® modelling, with possible extrapolation to reach the solar absorptivity. In this way, different tests have been made on micro-concrete at different solar fluxes, immerging thermocouples in depth: type S thermocouples have been immerged at 3 mm while type K thermocouples have been immerged at 6 and 9 mm. Figure IX shows results for the 3 mm depth thermocouple. Curves are plotted for different times: 15, 30, 60 and 90 seconds. Equilibrium temperature is reached after 120 seconds. A linear behaviour is observed between surface temperature and concentrated solar flux up to the smoke generation, i.e. for 6.5 MW/m^2 solar flux. In this domain, with a silica-based passive protective layer on the top of the sample, heat conduction is the most important phenomenon, with heat loss by convection and radiation. Increasing concentrated solar flux leads to a linear increase of the temperature inside the sample.

Similar behaviours are observed for the thermocouples located at 6 and 9 mm: above 6.5 MW/m^2, a linear behaviour is not observed anymore. To achieve material modelling, another approach has to be considered.

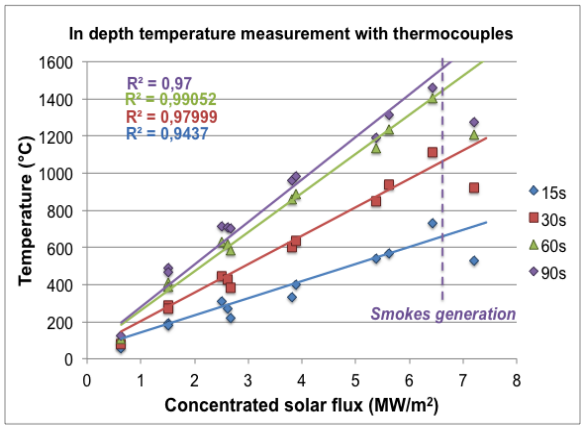

Fig. IX Temperature measured with thermocouples at 3 mm from the surface.

The hypothesis of constant temperature during transformation could be made: for concentrated solar fluxes higher than 6.5 MW/m^2 temperature is supposed to be constant, because of sublimation and oxidation transformations in the material. Each material transformation needs an amount of energy called latent heat of transformation. To evaluate this

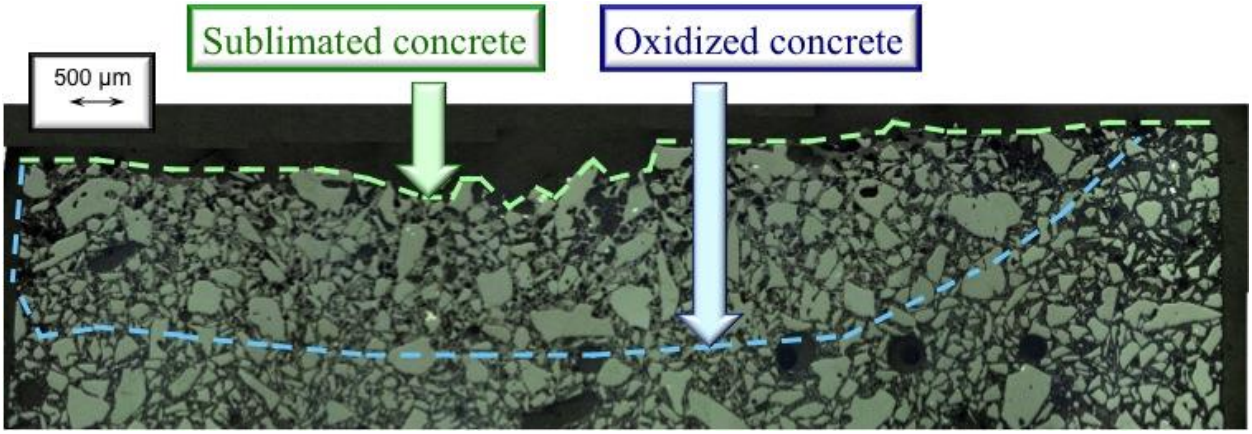

Fig. X Optical microscopy view of a micro-concrete polished specimen exposed to 9 MW/m^2 during 90 seconds (cross section).

energy, COMSOL® modelling is under study. The ratio between the transition value of the absorbed concentrated solar flux and the mass loss rate gives the amount of energy (J/kg) necessary to the material transformation.

III.IV Discussion

SEM and optical microscopy have been used to study ablation concrete behaviour. As an example, a cross section of a sample tested at 9 MW/m^2 during 90 seconds is shown in Figure X. Ablated material can be divided into two zones: the first one is characterized by sublimation, the second one by oxidation. Sublimation of concrete creates craters, more pronounced in the core of the sample. This differential behaviour is due to the Gaussian form of the concentrated solar flux. A second zone is located under this first one and corresponds to oxidized concrete.

Concrete oxidation is caused by oxygen diffusion through eutectic liquid phases and concrete porosities. In particular, bubbles are formed at the solid-gas interfaces because of SiO, Si and CO gases formation.

Figure XI shows the micro-concrete surface exposed to 15 MW/m^2 during 90 seconds. In the central zone, effects of active oxidation on SiC aggregates are visible (porous surface), while on the edges region, eutectic liquid phases cover the concrete surface.

Micro-cracks formed during concrete cooling, because of mismatch of thermal expansion coefficient between liquid phases, cement matrix and SiC aggregates. Bubbles are visible in cement liquid phase. Evaporation of CO and SiO gases formed during active oxidation of SiC aggregates is probably the cause of this phenomenon.

SiC aggregate after active oxidation at 11 MW/m^2 during 90 seconds is shown in figure XII. A liquid phase can be observed between the SiC aggregate and the vaporization zone. This liquid phase could come from cement eutectics or liquid silicon, formed at 1687°C from solid SiC [17].

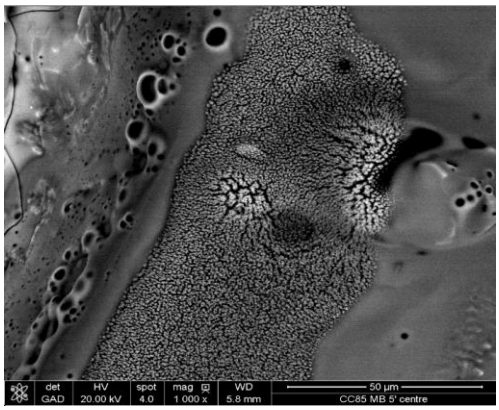

Fig. XI SEM image of micro-concrete exposed during 90 seconds at 15 MW/m^2.

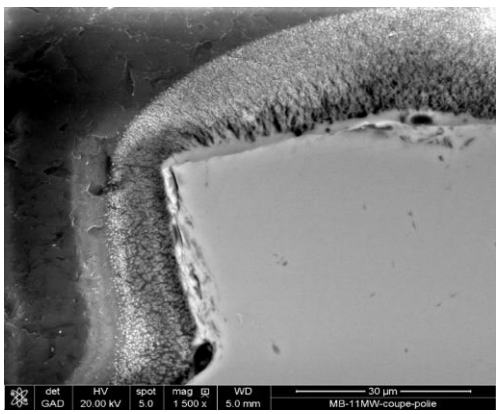

Fig. XII SEM image of micro-concrete (cross section): SiC aggregate after active oxidation at 11 MW/m^2 during 90 seconds.

IV. CONCLUSIONS/PROSPECTS

Micro-concrete oxidation has been studied using solar furnace facility, with concentrated solar fluxes up to 15 MW/m^2. The evolution of the mass loss is linear with time corresponding to active oxidation of the SiC aggregates. For concentrated solar flux higher than 6.5 MW/m^2, smokes generation occurs with SiO and CO emitted and this smoke prevents direct temperature measurement by optical pyrometry at 5 μm.

Pure silicon carbide has been oxidized at 7.5, 12 and 15 MW/m^2 during 30 seconds. Silica deposition has been observed for solar flux higher than 12 MW/m^2. Similar behaviour for micro-concrete has been observed. According to experimental results, after 30 seconds at 12 and 15 MW/m^2, mass loss for the micro-concrete is greatly smaller than that for pure α-type silicon carbide. This result is really interesting for future applications.

According to thermocouple measurements, a linear relation between surface temperature and concentrated solar flux exists. This result could lead to COMSOL® modelling of heat transfer in the material. Optimization loop could allow the calculation of the absorbed solar flux, solar absorptivity and surface temperature of the material. Validation will be made with direct measurements by optical pyrometry for concentrated solar flux lower than 6.5 MW/m^2. The ratio of the absorbed solar flux to the mass loss rate gives the latent heat of ablation of micro-concrete, which can be compared with the same value for SiC. Mass loss curves will be plotted versus surface temperature using this model. After this, MatLab® and Abaqus® ablation modelling will be possible.

Liquid phases, active oxidation and bubbling have been observed in the micro-concrete, with mass loss and oxygen diffusion in-depth into the material. Two zones have been observed by SEM during ablation: the sublimation zone with direct mass loss, and the oxidation zone, with bubbling and porosity rate increasing.

V. ACKNOWLEDGMENTS

Authors want to thank CNES and Midi-Pyrenees region for the financial support to the Ph.D. thesis. Authors thank Yannick Le Maoult for helpful discussions.

VI. REFERENCES

[1] C. Wagner, "Passivity during the Oxidation of Silicon at Elevated Temperatures," *Journal of Applied Physics*, vol. 29, no. 9, pp. 1295–1297, 1958.

[2] J. W. Hinze and H. C. Graham, "The Active Oxidation of Si and SiC in the Viscous Gas-Flow Regime," *Journal of The Electrochemical Society*, vol. 123, no. 7, pp. 1066–1073, 1976.

[3] P. C. Hewlett, *Lea's chemistry of cement and concrete*. 2001.

[4] W. E. Lee, W. Vieira, S. Zhang, G. K. Ahari, H. Sarpoolaky, and C. Parr, "Castable refractory concretes," *International Materials Reviews*, vol. 46, no. 3, pp. 145–167, 2001.

[5] "NF P-94-410-3 Essais pour déterminer les propriétés physiques des roches," *AFNOR*, 2001.

[6] CALDERYS, "TDS CCmicrobéton." 2011.

[7] A. Mazzoni, "Comportement thermomécanique d'un béton réfractaire : effets du renforcement par des fibres minérales," Université Paul Sabatier, Toulouse/Albi, 2009.

[8] ASTM, Ed., "Standard Test Method for Dynamic Young's Modulus, Shear Modulus, and Poisson's Ratio by Impulse Excitation of Vibration," *ASTM E1876-09*, 2009.

[9] L. Charpentier, K. Dawi, J. Eck, B. Pierrat, J.-L. Sans, and M. Balat-Pichelin, "Concentrated solar energy to study high temperature materials for space and energy," *Journal of solar energy engineering*, vol. 133, 2011.

[10] E. T. Turkdogan, P. Grieveson, and L. S. Darken, "Enhancement of diffusion-limited rates of vaporization of metals," *Journal of Physical chemistry*, 1952.

[11] A. H. Heuer and V. L. K. Lou, "Volatility Diagrams for Silica, Silicon Nitride, and Silicon Carbide and Their Application to High-Temperature Decomposition and Oxidation," *Journal of American Ceramic society*, vol. 73, no. 10, pp. 2789–2803, 1990.

[12] M. Balat, G. Flamant, G. Male, and G. Pichelin, "Active to passive transition in the oxidation of silicon carbide at high temperature and low pressure in molecular and atomic oxygen In the gaseous phase," *Journal of Materials Science*, vol. 27, pp. 697–703, 1992.

[13] M. Balat, “Determination of the Active-to-Passive Transition in the Oxidation of Silicon Carbide in Standard and Microwave-Excited Air,” *Journal of European Ceramic Society*, vol. 16, pp. 55–62, 1996.

[14] L. Charpentier, M. Balat-Pichelin, and F. Audubert, “High temperature oxidation of SiC under helium with low-pressure oxygen - Part 1 : Sintered alfa-SiC,” *Journal of European Ceramic Society*, vol. 30, pp. 2653–2660, 2010.

[15] L. Charpentier, M. Balat-Pichelin, H. Glénat, E. Bêche, E. Laborde, and F. Audubert, “High temperature oxidation of SiC under helium with low-pressure oxygen. Part 2 : CVD beta-SiC,” *Journal of European Ceramic Society*, vol. 30, pp. 2661–2670, 2010.

[16] K. Dawi, M. Balat-Pichelin, L. Charpentier, and F. Audubert, “High temperature oxidation of SiC under helium with low-pressure oxygen. Part 3 : beta-SiC-SiC/PyC/SiC,” *Journal of European Ceramic Society*, vol. 32, pp. 485–494, 2012.

[17] M. Jansen, *High performance non-oxide ceramics I*. 2002.